

Hexavalent chromium adsorption capability onto carbon black: kinetic and thermodynamic aspects

Rađenović, Ankica; Medunić, Gordana

Source / Izvornik: **Environmental Engineering and Management Journal, 2018, 17, 1931 - 1939**

Journal article, Published version

Rad u časopisu, Objavljena verzija rada (izdavačev PDF)

Permanent link / Trajna poveznica: <https://um.nsk.hr/um:nbn:hr:115:375151>

Rights / Prava: [In copyright](#) / [Zaštićeno autorskim pravom.](#)

Download date / Datum preuzimanja: **2025-02-25**



SVEUČILIŠTE U ZAGREBU
METALURŠKI FAKULTET
UNIVERSITY OF ZAGREB
FACULTY OF METALLURGY

Repository / Repozitorij:

[Repository of Faculty of Metallurgy University of Zagreb - Repository of Faculty of Metallurgy University of Zagreb](#)





“Gheorghe Asachi” Technical University of Iasi, Romania



HEXAVALENT CHROMIUM ADSORPTION CAPABILITY ONTO CARBON BLACK: KINETIC AND THERMODYNAMIC ASPECTS

Ankica Radjenovic^{1*}, Gordana Medunic²

¹University of Zagreb, Faculty of Metallurgy, Aleja narodnih heroja 3, 44000 Sisak, Croatia

²University of Zagreb, Faculty of Science, Department of Geology, Horvatovac 95, 10000 Zagreb, Croatia

Abstract

The adsorption rate and dynamic behavior of the system are important factors as regards the process design and operational control. The aim of this study was to find a suitable kinetic model for the hexavalent chromium removal in a batch reactor. The experimental data were analyzed using four adsorption kinetic models: the pseudo- first and second order equations, the Elovich equation, and the intraparticle diffusion equation, so as to determine the best fit equation of the Cr(VI) adsorption onto the carbon black. The rate constants and the related correlation coefficients for the each kinetic model were calculated and discussed. Also, the predicted $q_{e,cal}$ values from the kinetic equations were compared with the experimental data. The results showed that the pseudo-second order equation provided the best correlation of the adsorption process ($R^2 = 0.9820 - 0.9978$), whereas the Elovich equation also fitted well with the experimental data ($R^2 = 0.9561 - 0.9599$). The corresponding rate constants corresponded to values $0.0144 - 0.0205$ g/mg min. Analyses were performed at 293, 313, and 333 K. Based on the rate constants, obtained by the kinetic model using the Arrhenius and Eyring equations, the activation parameters were determined, i.e. the activation energy (4.37 kJ/mol), the change of entropy (273.74 J/mol K), enthalpy (- 1.79 kJ/mol), and the Gibbs free energy (- 1.78 kJ/ mol).

Key words: carbon black, Cr(VI) adsorption, kinetics, thermodynamics

Received: March, 2014; *Revised final:* September, 2014; *Accepted:* October, 2014; *Published in final edited form:* August, 2018

1. Introduction

Recently, the levels of several toxic metals in waters have been increasing gradually due to the pollution caused by industrial and municipal wastewater discharges. Chromium is heavy metal commonly found in high levels in wastewater discharges from various industries. The main industrial activities that cause chromium pollution are electroplating, mining, metal finishing, leather tanning, electrical and electronic equipment, catalysis, pigments, chemical manufacturing etc. (Bradl et al., 2005). Chromium is characterized by beneficial as well as detrimental properties. Cr(III) is a less toxic form which can be readily precipitated out of solution in the form of $\text{Cr}(\text{OH})_3$. At low concentrations it can be considered a bioelement since it plays an important

role in the metabolism of plants and animals (Barrera-Díaz et al., 2012; Mohan and Pittman, 2006). On the other hand, Cr(VI) ions are 500 times more toxic than the trivalent version. Cr(VI) species are known to be toxic and carcinogenic, causing health problems such as liver damage, pulmonary congestions, vomiting, and severe diarrhea. Eye exposure to hexavalent form may result in its permanent damage. Chromium(VI), which is primarily present in the form of chromate (CrO_4^{2-}) and dichromate ($\text{Cr}_2\text{O}_7^{2-}$), has significantly higher levels of toxicity than the other valence states. Hence, governments apply the enhanced regulation for chromium species. In Croatia, the upper limit for the discharge of Cr(VI) into the inland surface waters and public drainage systems is 0.1 mg/L (OG, 2008).

The adsorption process has been found to be more effective and cheaper as regards the treatment of

* Author to whom all correspondence should be addressed: e-mail: radenova@simet.hr; Phone: +38544533378; Fax: +38544533378

wastewaters compared to other methods (Fu and Wang, 2011). While aiming at cheaper adsorbents applicable in small scale industries, many researchers have made use of low-cost adsorbents for the chromium ion removal. They include agricultural by-products, such as sawdust, coir pith, rice bran, nut shells, cork powder, leaf mould, wheat bran, bark and biosorbents algae, fungi, plants, and bacteria. The Cr(VI) adsorptive removal from water by the industrial by-products and/or wastes has been tested so far (e.g. fly ash, blast furnace slag, red mud, waste tires, waste sludge) (Barrera-Díaz et al., 2012; Dhal et al., 2013; Mohan and Pittman, 2006; Rafatullah et al., 2009; Srivastava et al., 2017; Sud et al., 2008).

Increasing concern with the Cr(VI) pollution has significantly urged the investigation and development of the newly improved materials to address these problems. Carbon black (CB) is a type of carbon material with widespread applications, such as reinforcing compounds in rubbers, electrically conductive agents in plastics, and as catalyst support in proton exchange membrane fuel cells (Ban et al., 2011). Based on the literature survey, it can be said that a commercial CB has not been tested as an adsorbent of the Cr(VI) ions from aqueous solutions.

In the present work, the adsorption kinetics and thermodynamics of the hexavalent chromium adsorption onto the commercial CB were studied. The four kinetic models were applied on the experimental data and the associated parameters were evaluated. The CB was characterized so as to understand the nature of an adsorbate/adsorbent interaction.

2. Material and methods

2.1. Adsorbent characterization

The commercial CB was produced by oil furnace process. Raw materials were the aromatic oil derivatives produced by the secondary petroleum refining processes. The CB samples were dried at 105°C for 2 hours and sieved to particle size from 0.09 to 0.125 mm. The composition of the CB was as follows: 97.6% C, 0.4% H, 1.02% O, and 0.98% S.

The Fourier transform infrared spectroscopy (FT-IR) analysis was used to identify the surface functional groups of the CB sample in the range from 4000 to 650 cm^{-1} using the Spectrum One FTIR spectrometer, Perkin Elmer (UK). The sample was characterized in its basic form without any preparation, using the attenuated total reflectance (ATR) chamber. The surface area properties were determined by the Brunauer-Emmett-Teller (BET) and Barrett-Joyner-Halenda (BJH) methods using a Micromeritics ASAP 2000 (USA) adsorption instrument. The average pore diameter was calculated according to the equation (Eq. 1):

$$d = \frac{4 \cdot V_p}{S_p} \quad (1)$$

where V_p is specific volume, and S_p is specific surface area. Pore size distribution of the CB was calculated by the Barrett-Joyner-Halenda (BJH) method. Microscopic observation was performed using a scanning electron microscope (SEM) Tescan Vega TS 5136 MM (Czech Republic) by the Bruker energy-dispersive spectrometer (EDS) by point analysis.

2.2. Adsorption kinetics

The removal of chromium ions was studied by the batch tests. Prior to experiments, a stock solution of hexavalent chromium of target concentration was prepared by dissolving an appropriate amount of $\text{K}_2\text{Cr}_2\text{O}_7$ in deionized water. The test solutions were prepared from the stock solution according to the relevant dilution.

Subsequently, 0.25 g of the CB sample was mixed with 50 ml of 50, 100, and 200 mg/L of the Cr(VI) solutions during 15 to 120 minutes at 293, 313, and 333 K. Following the completion of the experiments, the suspension was filtered through a Whatman filter paper No. 44. The Cr(VI) concentration in the supernatant was analyzed by the Camspec M-107, Jencons (UK) spectrophotometer at 540 nm. The optimal ratio of the adsorbent/adsorbate (0.25g/50 mL) and pH of the solution (2.4) were determined during the previous experiments (Radjenovic and Medunic, 2015). The experimental results showed that the equilibrium contact time was obtained within 75 min, and the maximum adsorption capacity was 33.22 mg/g.

To check the analytical reproducibility during the concentration measurements, the experiments were run in triplicate under identical conditions, and the average values are reported.

3. Results and discussion

3.1. Characterization of the carbon black

The FTIR analysis provides the information on the surface chemistry of the examined samples (Fig. 1). The CB sample exhibited some characteristic peaks, at the wavenumbers of 2357 and 2324 cm^{-1} which were associated with carbonyl groups in R-(C=O)-R'. The peak at 2100 cm^{-1} was attributed to the stretching vibrations of C=C.

The adsorbent capacity to adsorption of metal ions depend on the quantity of surface functional groups (Chen et al., 2010; Li et al., 2007). Carbon atoms of the CB, either localized at the edges and the periphery of the aromatic sheets or those located at the defect positions, were associated with an unpaired electron or they had residual valences, hereby posing high potential energy. These carbon atoms were more reactive and had a tendency to form the surface oxygen complexes. Such surface chemical groups may promote the chromium(VI) adsorption (Kothiyal and Sharma, 2013).

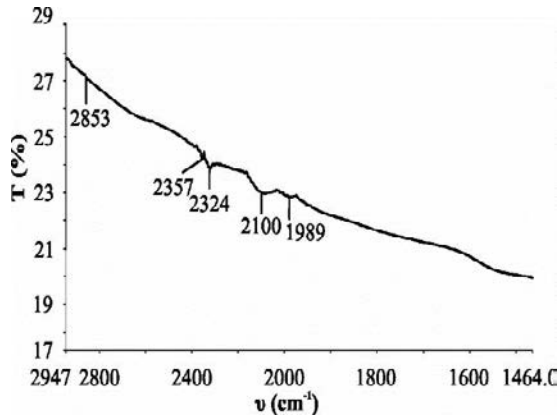


Fig. 1. FTIR spectra of the carbon black (CB).

The adsorption phenomenon depends on the interaction between the surface of an adsorbent and adsorbed species. The characteristic values of the CB surface area properties were as follows: the BET surface area, $S_{BET} = 107.29 \text{ m}^2/\text{g}$, the total pore volume (1.7-300 nm), $V_p = 743 \cdot 10^{-3} \text{ cm}^3/\text{g}$, and the average

pore diameter, $d = 16.99 \text{ nm}$. This surface area value could be explained by fine grained particle size of the CB and their porous nature. According to the IUPAC, the pores of a porous material are classified into three groups: micropores (width $d < 2 \text{ nm}$), mesopores ($2 \text{ nm} < d < 50 \text{ nm}$), and macropores ($d > 50 \text{ nm}$). On the basis of the obtained results, the CB may be considered a mesoporous material (Srinivasan and Yaming, 2001).

Fig. 2a shows SEM image of the CB sample surface prior to the adsorption with clearly visible, mostly rounded particles, of various sizes though. The aggregates were formed by a coalescence of elemental particles. The fusion of the aggregates by Van der Waals forces resulted in the formation of the new structures – agglomerates, as previously described in literature (Ban et al., 2011; Radjenovic and Malina, 2013). The changes caused by the Cr(VI) ion adsorption as accumulations and deposits are shown in Fig. 2b. Fig. 3 depicts the EDS spectra. Following the Cr(VI) ion adsorption, it was evident that the surfaces contained chromium (Fig. 3b).

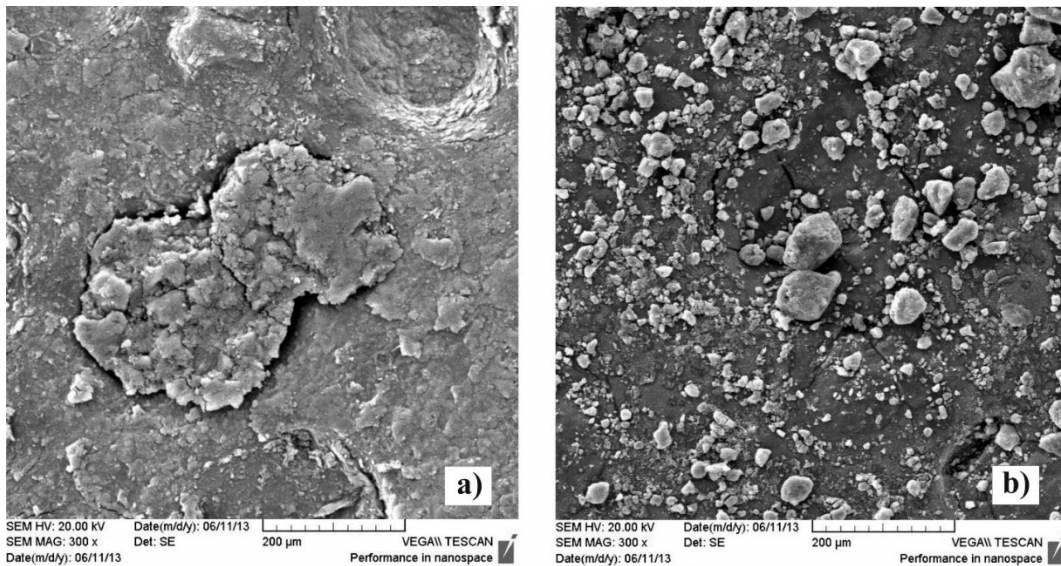


Fig. 2. SEM image of the CB surface, a) prior, and b) following the Cr(VI) adsorption ($c_i = 200 \text{ mg/L}$)

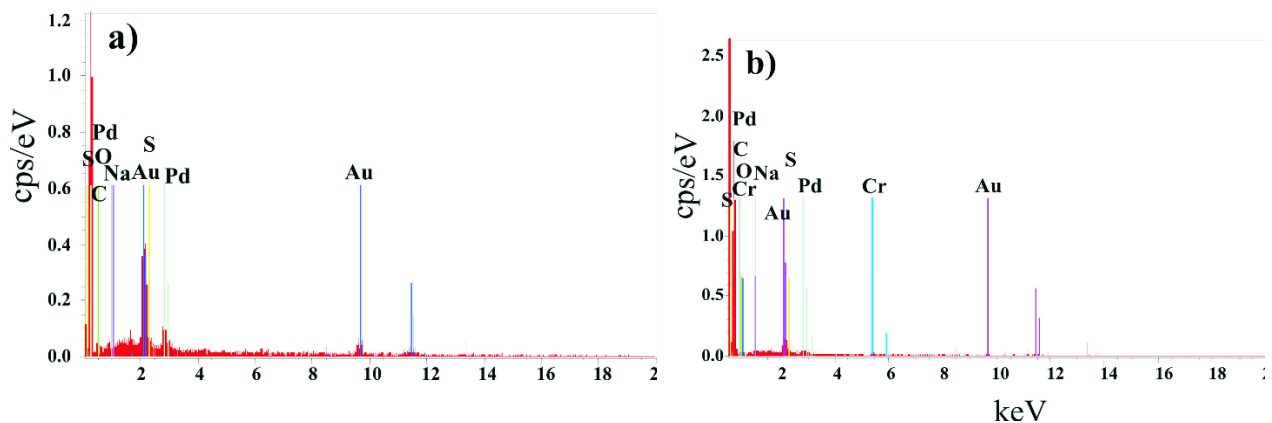


Fig. 3. EDS spectra of the carbon black a) prior, and b) following the Cr(VI) adsorption ($c_i = 200 \text{ mg/L}$)

3.2. Adsorption kinetics study

The adsorption isotherms represent the relationship between an amount adsorbed by unit weight of a solid adsorbent and the amount of a solute remaining in the solution at an equilibrium and at the constant temperature (Ho et al., 2002). The amount adsorbed at an equilibrium, i.e. the adsorption capacity, q_e (mg/g) was calculated according to the formula (Eq. 2):

$$q_e = \frac{\Delta c}{m} \cdot V \tag{2}$$

where Δc is quantity of an adsorbed adsorbate ($\Delta c = c_i - c_e$), mg/L; c_i is the initial concentration of an adsorbate, mg/L; c_e is the equilibrium concentration of an adsorbate, mg/L; V is volume of solution, L; and m is adsorbent mass, g.

The equilibrium adsorption isotherm of the Cr(VI) ions onto the CB is shown in Fig. 4. It can be seen that the Cr(VI) ion adsorption increases with an increase of the initial Cr concentration, while decreasing with the rise in temperature. The amounts of oxygen functional groups, such as carbonyl groups, resulted in an increase of the surface cation exchange and complexation capacity of the CB (Kothiyal and Sharma, 2013; Radjenovic and Malina, 2013).

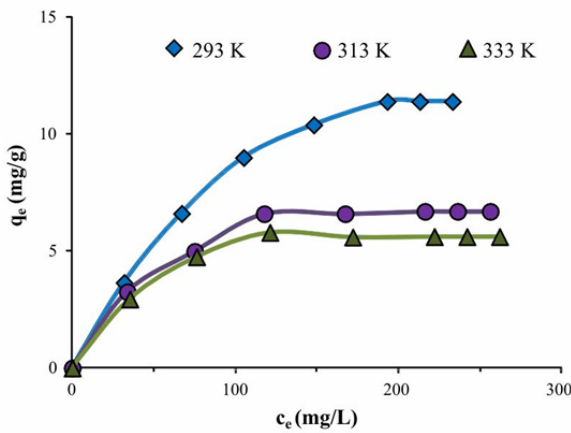


Fig. 4. Equilibrium adsorption isotherm of Cr(VI) onto the CB

Results of the effect of the equilibrium time on the adsorption of Cr(VI) by the CB is shown in Fig. 5. It is evident that the Cr removal takes place in two steps: a relatively fast phase continuing up to 30 min followed by a slow progress until the state of equilibrium (75 min). The high initial uptake rate is due to availability of a large number of adsorption sites at the onset of the process. The sticking probability is also high on the bare surface accounting for the high adsorption rate. Furthermore, the CB is exclusively mesoporous, hence the diffusion of solute into the pores appears to be easier (Borah et al., 2009). The faster solute removal as well as the low equilibration time is attributed to highly favourable

adsorptive interactions. Following the 30 minute period, occupation of the remaining vacant surface sites was difficult due to repulsive forces among chromium(VI) ions adsorbed on the adsorbent surface and the ones in solution in the form of HCrO_4^- , $\text{Cr}_2\text{O}_7^{2-}$, and CrO_4^{2-} ions (Fu and Wang, 2011; Mohan and Pittman, 2006).

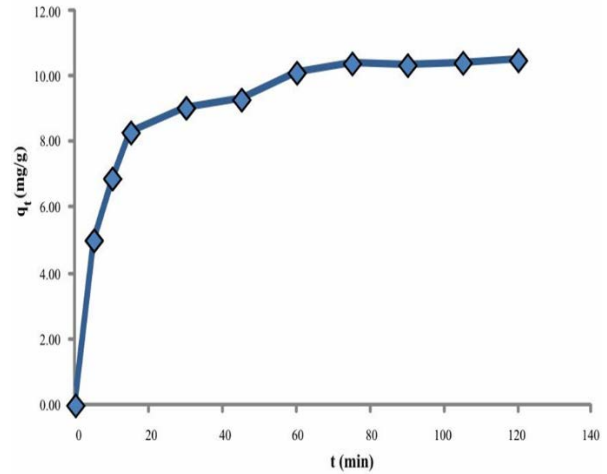


Fig. 5. Results of the Cr(VI) adsorption capacity onto the CB vs. time

In order to examine the adsorption process mechanism, such as mass transfer and chemical reaction, a suitable kinetic model was needed to analyze the rate data.

The adsorption kinetics may be described by the pseudo-first order kinetic model given by Lagergren. The linear pseudo-first order equation (Eq. 3) is as follows (Lagergren, 1898):

$$\ln(q_e - q_t) = \ln q_e - k_1 \cdot t \tag{3}$$

where q_e and q_t are the amounts of an adsorbate adsorbed at the equilibrium and at time t (mg/g), respectively, whereas k_1 is the equilibrium rate constant of the pseudo-first order adsorption, (1/min).

The slopes and intercepts of the plots of $\log(q_e - q_t)$ versus t were used to determine the first-order rate constant k_1 and the equilibrium adsorption capacity, q_e (Fig. 6a). The values of $q_{e,exp}$, k_1 , the theoretic values $q_{e,cal}$ and the correlation coefficient R_1^2 are all listed in Table 1. It can be seen that the correlation coefficients are not high ($R_1^2 = 0.9121 - 0.9421$), whereas the agreement between $q_{e,cal}$ and $q_{e,exp}$ is also not good.

Table 1. Parameters of the pseudo first-order kinetic model

c_i (mg/L)	$q_{e,exp}$ (mg/g)	$q_{e,cal}$ (mg/g)	k_1 (1/min)	R_1^2
50	3.654	4.462	0.0497	0.9421
100	6.610	4.921	0.0470	0.9121
200	10.450	5.670	0.0462	0.9303

The adsorption kinetics may also be described by the pseudo-second order equation. The pseudo-second order equation (Eq. 4) in integrated form is as follows (Kara and Demirel, 2012).

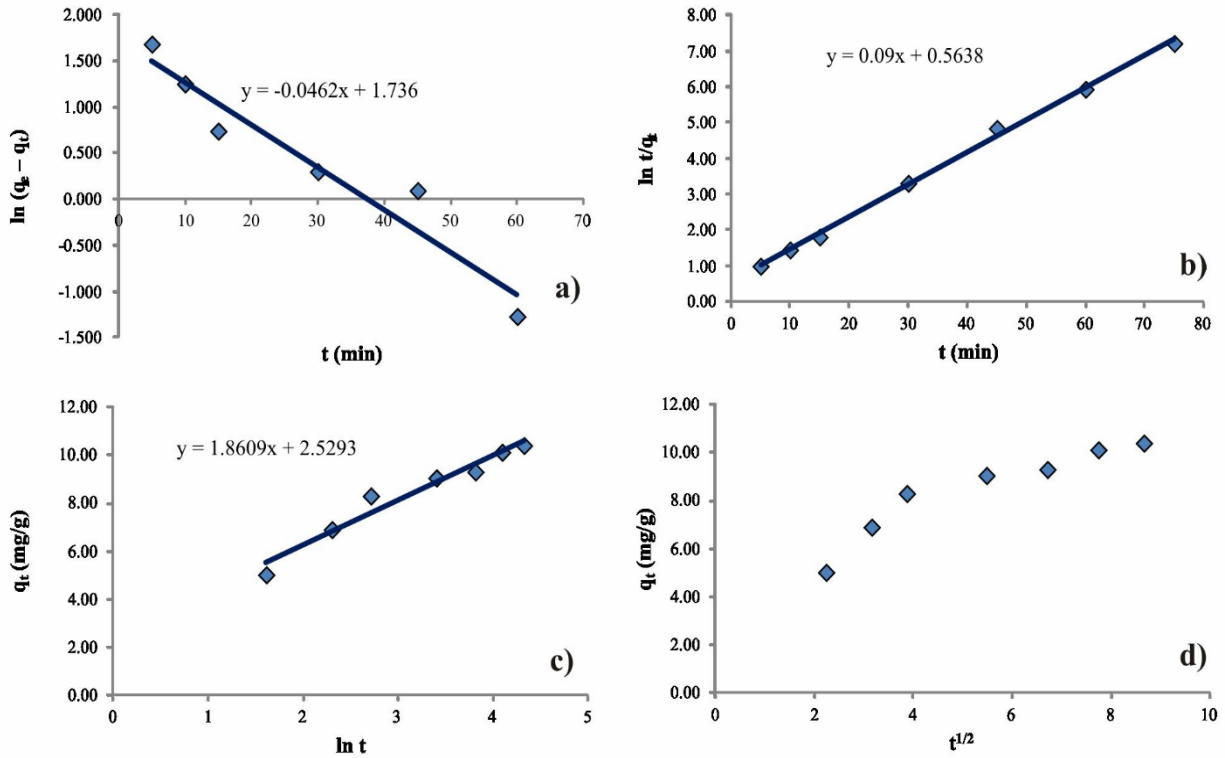


Fig. 6. Kinetic model for the adsorption of Cr(VI) ions ($c_i = 200$ mg/L) onto the CB: a) pseudo first-order model, b) pseudo second-order model, c) Elovich model, and d) intraparticle diffusion model

$$\frac{t}{q_t} = \frac{1}{k_2 \cdot q_e^2} + \frac{t}{q_e} \quad (4)$$

where k_2 is the equilibrium rate constant of the pseudo-second order adsorption reaction (g/mg min). The slopes and intercepts of the plots t/q_t versus t were used to calculate the second-order rate constants k_2 (Fig. 6b). The initial adsorption rate, h_0 (mg/g min) was defined (Eq. 5) as follows (Yao et al., 2010):

$$h_0 = k_2 q_e^2 \quad (5)$$

For all experimental concentrations, the R_2^2 values were close to 1; there was a little difference between $q_{e,exp}$ and $q_{e,cal}$ (Table 2). Also, it can be seen from Table 3 that with an increase in initial chromium concentration, the initial adsorption rate, h_0 increases, while the rate constant of the adsorption k_2 decreases.

Table 2. Parameters of the pseudo second-order kinetic model

c_i (mg/L)	$q_{e,exp}$ (mg/g)	$q_{e,cal}$ (mg/g)	k_2 (g/mg min)	h_0 (mg/g min)	R_2^2
50	3.654	4.049	0.0205	0.0915	0.9820
100	6.610	6.243	0.0183	0.1142	0.9901
200	10.450	11.110	0.0144	0.1598	0.9978

The pseudo-second order model is based on the assumption that the rate-limiting step may be a chemical nature involving the valence forces through the sharing or exchange of electrons between an

adsorbent and an adsorbate. This model, contrary to the pseudo-first order model, adequately predicts the adsorption behaviour over the whole adsorption period.

The Elovich equation assumes that the solid surface active sites are heterogeneous in nature, and therefore exhibit different activation energies for chemisorption. The linear Elovich equation (Eq. 6) is given as follows (Aharoni and Tompkins, 1970):

$$q_t = 1/\beta \ln(\alpha\beta) + 1/\beta \ln t \quad (6)$$

where α is the initial adsorption rate (mg/g min), while β is related to the extent of surface coverage and the activation energy of chemisorption (g/mg). The Elovich kinetic constants, α and β , were obtained from the intercept and slope of the plot q_t versus $\ln t$ (Fig. 6c). The linear relationship was obtained among the adsorbed Cr(VI) ions, q_t and $\ln t$ over the entire adsorption period, with the correlation coefficients between 0.9561 and 0.9599 (Table 3). The α values were found to increase with an increase in initial Cr(VI) concentrations due to higher driving force. The constant β value decreased with an increase in initial Cr(VI) concentrations since less surface was available for the Cr(VI) ion adsorption.

Table 3. Parameters of the Elovich kinetic model

c_i (mg/L)	α (mg/g min)	β (g/mg)	R_2^2
50	5.3387	0.7965	0.9590
100	6.2120	0.6899	0.9599
200	7.2442	0.5374	0.9561

The adsorption mechanism of an adsorbate onto the adsorbent may involve one or more steps, e.g. via film or external diffusion, intra-particle diffusion or pore diffusion, surface diffusion and the adsorption on the pore surface, or a combination of more than one step.

Weber and Morris (1963) proposed the empirically established functional relationship stating that if an intraparticle diffusion is the rate-controlling factor, then an uptake varies with the square root of time. To elucidate the diffusion mechanism, the kinetic results were analyzed by the intra-particle diffusion model (Eq. 7) expressed as follows (Weber and Morris, 1963):

$$q_t = k_{id}t^{1/2} \quad (7)$$

where k_{id} is the intra-particle diffusion rate constant ($\text{mg/g min}^{1/2}$).

In an aqueous solution, as regards the adsorption onto the porous adsorbents, mesopores act as micropores possibly due to water layers formed on the pore walls (Ünlü and Ersoz, 2007). It is known that a pore and surface area play important role during the adsorption process. Since the CB has a porous structure, the effect of intra-particle diffusion to the adsorption process should be taken into account.

If the Weber–Morris plot of q_t versus $t^{1/2}$ is linear and passes through the origin, then the adsorption process is controlled only by the intra-particle diffusion (Borah et al., 2009). It can be seen that the relationship was not linear for the entire reaction time range. The plot shows two parts (Fig. 5d); the first linear part represents the initial rapid uptake due to film diffusion and a consequent external surface coverage by an adsorbate. The second portion represented the gradual adsorption stage where intra-particle diffusion is the rate limiting factor. The rate parameters, k_{id} , together with the correlation coefficients are listed in Table 4. As can be seen from Fig. 5 and Tables 1-4, the pseudo-second order

equation provides the best correlation as regards the adsorption process, whereas the Elovich equation also fitted well in the experimental data. However, the pseudo-first order and the intraparticle diffusion equations did not fit well with the experimental data as regards the Cr(VI) adsorption. This feature suggested that the investigated adsorption systems belonged to the second-order kinetic model. Rationale is the assumption that the rate limiting step might be the chemical reaction involving the valency forces through the sharing or exchange of electrons between an adsorbent and an adsorbate (Örnek et al., 2007).

These results are consistent with the CB's mesoporous nature having various fractions of micro- and macro-pores. Namely, the first linear portion was attributed to a macropore diffusion process, while the second portion could be ascribed to a micropore diffusion process.

Table 4. Parameters of the intraparticle diffusion kinetic model

c_i (mg/L)	k_{id} (mg/g min ^{1/2})	R_{id}^2
50	0.5224	0.9672
100	0.5943	0.9471
200	0.7383	0.8769

The pseudo-first and pseudo-second order kinetic models are commonly used models for studies of the adsorption kinetics, and quantifications of the relevant uptake extent. Table 5 presents several kinetic models and the Cr(VI) adsorption capacities of various adsorbents.

3.3. Adsorption thermodynamics study

The type of the adsorption mechanism, either physical or chemical, can be evaluated by calculating the activation energy and the thermodynamic parameters. The rate constant of the saturation type of an adsorption reaction (k_1 or k_2) is expressed as a function of temperature by the following Arrhenius type (Eq. 8) relationship (Atkins and De Paula, 2006).

Table 5. Comparison of kinetic models and the Cr(VI) adsorption capacities of various adsorbents

Adsorbent	Kinetic model	Maximum adsorption capacity, mg/g	Reference
Activated coconut shell carbon	pseudo-first order	-	Ho et al. (2000)
Activated neem leaves	pseudo-second order	62.97	Babu and Gupta (2008)
Banana peel	pseudo-first order and Reichenberg	131.56	Memon et al. (2009)
Carbon black (derived from wheat-residue)	pseudo-second order	21.34	Wang et al. (2010)
Carbon anode dust	intraparticle diffusion	2.00	Štrkalj et al. (2010)
Chitosan	pseudo-second order	102.00	Aydin and Aksoy (2009)
Commercial activated carbon	pseudo-second order	200.00	Kothiyal and Sharma (2013)
Copper coated moss	pseudo-first order	-	Ho et al. (2000)
Modified wheat residue	pseudo-second order and intraparticle diffusion	322.58	Chen et al. (2010)
Treated sawdust	pseudo-second order	9.55	Baral et al. (2006)
Carbon black	pseudo-second order (this study)	33.22	Radjenovic and Medunic (2015)

$$k = A \exp(-E_a/RT) \quad (8)$$

where k is the rate constant, A is the frequency factor, E_a is the activation energy of the process (kJ/mol), R is the universal gas constant (J/mol K), and T is the solution temperature (K). The fact that E_a is given by the slope of the plot of $\ln k_2$ against $1/T$ points out that as the activation energy gets higher, the temperature dependence of the rate constants gets stronger. The $\ln k_2$ values were plotted against $1/T$ (Fig. 7) and the activation energy was calculated to be 4.37 kJ/mol. It can be concluded that the rate constant of the Cr(VI) adsorption onto the CB does not substantially depend on the temperature.

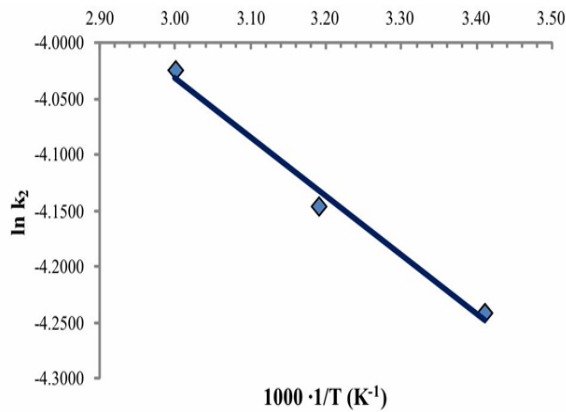


Fig. 7. Arrhenius plot

The activation entropy and enthalpy were evaluated according to the Eyring equation (Eq. 9), as dependence of the constant rate on temperature (Holleman and Wiberg, 2001):

$$\ln(k_2/T) = \ln(k_b/h) + (\Delta S^*/R) - (\Delta H^*/RT) \quad (9)$$

where k_2 is the rate constant, k_b is the Boltzmann constant (J/K), h is the Planck's constant (J/s), ΔH^* is the enthalpy of activation (kJ/mol), and ΔS^* is the entropy of activation (J/mol K). The enthalpy of activation, ΔH^* was calculated from the slope of a linear dependence ($-\Delta H^*/R$) of $\ln(k_2/T)$ versus $1/T$ plot (Fig. 8), whereas the entropy of activation ΔS^* was calculated from the intercept [$\ln(k_b/h) + (\Delta S^*/R)$]. The free energy of activation was as follows (Eq. 10):

$$\Delta G^* = \Delta H^* - T \Delta S^* \quad (10)$$

The values of ΔH^* and ΔS^* of the adsorption process were -1.79 kJ/mol and 273.74 J/molK (Table 6), respectively. The negative value of the enthalpy reflects the exothermic nature of the adsorption process. To a certain extent, physisorption and chemisorption can be classified by the magnitude of the enthalpy change. Bonding strengths of <84 kJ/mol are commonly considered as those of the physisorption bonds (Atkins and De Paula, 2006). The obtained thermodynamic parameter values, including the activation energy, suggest that the physisorption was dominant as regards the Cr(VI) adsorption onto

the CB. The positive ΔS^* value corresponded to an increase in the degrees of freedom of the solid-liquid interface during the adsorption of Cr(VI) ions onto the CB, supporting the ion-exchange adsorption mechanism (Chen et al., 2010).

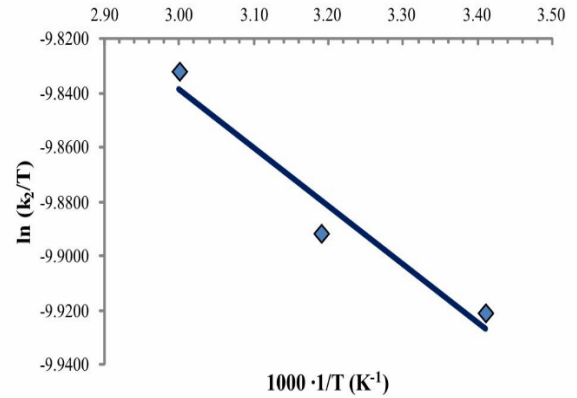


Fig. 8. Plot of $\ln(k_2/T)$ vs. $1/T$

Table 6. Thermodynamic parameters of the Cr(VI) adsorption onto the CB

E_a , kJ/mol	ΔH^* , kJ/mol	ΔG^* , kJ/mol	ΔS^* , J/mol K
4.37	- 1.79	- 81.78	273.74

The ΔG^* values were found to be negative, thus indicating that the adsorption process was spontaneous and thermodynamically favorable.

4. Conclusions

Kinetic parameters showed that the adsorption of dissolved chromium onto the CB was controlled mainly by the pseudo-second order equation. The values of the activation enthalpy and entropy gave evidence of the exothermic character. The negative activation free energy confirmed the spontaneity of the adsorption process. The obtained thermodynamic parameter values, including the activation energy, suggest that the physisorption was dominant during the Cr(VI) adsorption onto the CB.

It can be concluded that the CB may be used for the removal of hexavalent chromium ions by the batch procedure, thus acting as an alternative to more costly adsorbents.

List of abbreviations

$1/b$ – adsorption potential of the adsorbent
 B – Temkin constant
 BET – Brunauer-Emmett-Teller
 BJH – Barrett-Joyner-Halenda
 CB – Carbon Black
 c_e – equilibrium concentration of chromium ions in the solution (mg/L)
 c_i – initial concentration of chromium ions in the solution (mg/L)
 c_t – concentration of chromium ions in the solution at time t (mg/L)

d – pore volume (nm)
 E_a – activation energy (kJ/mol)
 EDS – energy dispersive X-ray spectroscopy
 FTIR – Fourier transform infrared spectroscopy
 h – Planck's constant (J/s)
 k_1 – rate constant of pseudo first-order reaction (1/min)
 k_2 – rate constant of pseudo second-order reaction (g/mg min)
 k_b – Boltzmann constant (J/K)
 K_F, n – Freundlich constants
 k_{id} – intra-particle diffusion rate constant (mg /g min^{1/2}).
 K_L – Langmuir constant (L/mg)
 K_t – equilibrium binding constant corresponding to the maximum binding energy (L/mg)
 m – adsorbent mass (g)
 q_e – equilibrium adsorption capacity (mg/g)
 q_{max} – theoretical maximum adsorption capacity (mg/g)
 R – universal gas constant (J/mol K)
 R^2 – correlation coefficient
 S_{BET} – BET surface area (m²/g)
 SEM – Scanning electron microscopy
 T – absolute temperature (K)
 t – time (min)
 V – volume of the solution (L)
 V_p – total pore volume (cm³/g)
 α and β – Elovich constants
 Δc – quantity of chromium ions adsorbed (mg/L)
 ΔG^* – free energy change (kJ/mol)
 ΔH^* – enthalpy change (kJ/mol)
 ΔS^* – entropy change (J/molK)

Acknowledgements

This work was supported by the Ministry of Science, Education, and Sports of the Republic of Croatia, under the project 124-1241565-1524.

References

- Aharoni C., Tompkins F.C., (1970), *Kinetics of Adsorption and Desorption and the Elovich Equation*, In: *Advances in Catalysis and Related Subjects*, Eley D.D., Pines H., Weisz P.B. (Eds.), Academic Press, New York, 1-49.
- Atkins P., De Paula J., (2006), *Physical Chemistry*, WH Freeman and Comp., Oxford.
- Aydin Y., Aksoy N.D., (2009), Adsorption of chromium on chitosan: Optimization, kinetics and thermodynamics, *Chemical Engineering Journal*, **151**, 188-194.
- Babu B.V., Gupta S., (2008), Adsorption of Cr(VI) using activated neem leaves: kinetic studies, *Adsorption*, **14**, 85-92.
- Ban S., Malek K., Huang C., Liu Z., (2011), A molecular model for carbon black primary particles with internal nanoporosity, *Carbon*, **49**, 3362-3370.
- Baral S.S., Das S.N., Rath P., (2006), Hexavalent chromium removal from aqueous solution by adsorption on treated sawdust, *Biochemical Engineering Journal*, **31**, 216-222.
- Barrera-Díaz C.E., Lugo-Lugo V., Bilyeu B., (2012), A review of chemical, electrochemical and biological methods for aqueous Cr(VI) reduction, *Journal of Hazardous Materials*, **223-224**, 1-12.
- Borah D., Satokawa S., Kato S., Kojima T., (2009), Sorption of As(V) from aqueous solution using acid modified carbon black, *Journal of Hazardous Materials*, **162**, 1269-1277.
- Bradl H.B., Kim C., Kramar U., Stüben D., (2005), *Interactions of Heavy metals*, In: *Heavy Metals in the Environment: Origin, Interaction and Remediation*, Bradl H.B. (Ed.), Elsevier Ltd., London, 104-107.
- Chen S., Yue Q., Gao B., Xu X., (2010), Equilibrium and kinetic adsorption study of the adsorptive removal of Cr(VI) using modified wheat residue, *Journal of Colloid and Interface Science*, **349**, 256-264.
- Dhal B., Thatoi H.N., Das N.N., Pandey B.D., (2013), Chemical and microbial remediation of hexavalent chromium from contaminated soil and mining/metallurgical solid waste: A review, *Journal of Hazardous Materials*, **250-251**, 272-291.
- Fu F., Wang Q., (2011), Removal of heavy metal ions from wastewaters: A review, *Journal of Environmental Management*, **92**, 407-418.
- Ho Y.S., Ng J.C.Y., McKay G., (2000), Kinetics of pollutant sorption by biosorbents: review, *Separation and Purification Methods*, **29**, 189-232.
- Ho Y.S., Porter J.F., McKay G., (2002), Equilibrium isotherm studies for the sorption of divalent metal ions onto peat: copper, nickel and lead single component systems, *Water Air and Soil Pollution*, **141**, 1-33.
- Holleman A.F., Wiberg E., (2001), *Inorganic Chemistry*, Academic Press, San Diego.
- Kara A., Demirbel E., (2012), Kinetic, isotherm and thermodynamic analysis on adsorption of Cr(VI) ions from aqueous solutions by synthesis and characterization of magnetic-poly (divinylbenzene-vinylimidazole) microbeads, *Water Air and Soil Pollution*, **223**, 2387-2403.
- Kothiyal A.C., Sharma S., (2013), Study of chromium(VI) adsorption using pterispermum acerifolium fruit capsule activated carbon (FCAC) and commercial activated charcoal (CAC) as selective adsorbents, *The Holistic Approach to Environment*, **3**, 63-82.
- Lagergren S., (1898), About the theory of so-called adsorption of soluble substances (in German), *Kungliga Svenska Vetenskaps-Akademiens Handlingar*, **24**, 1-39.
- Li Q., Zhai J., Zhang W., Wang M., Zhou J., (2007), Kinetic studies of adsorption of Pb(II), Cr(III) and Cu(II) from aqueous solution by sawdust and modified peanut husk, *Journal of Hazardous Materials*, **141**, 163-167.
- Memon J.R., Memon S.Q., Bhangar M.I., El-Turki A., Hallam K.R., Allen G.C., (2009), Banana peel: A green and economical sorbent for the selective removal of Cr(VI) from industrial wastewater, *Colloids and Surfaces B: Biointerfaces*, **70**, 232-237.
- Mohan D., Pittman Jr C.U., (2006), Activated carbons and low cost adsorbents for remediation of tri- and hexavalent chromium from water, *Journal of Hazardous Materials*, **137**, 762-781.
- OG, (2008), Ordinance on limit values of hazardous and other substances in wastewater (in Croatian), *Official Gazette No. 94/2008*.
- Örnek A., Özacar M., Şengil İ.A., (2007), Adsorption of lead onto formaldehyde or sulphuric acid treated a corn waste: Equilibrium and kinetic studies, *Biochemical Engineering Journal*, **37**, 192-200.
- Radjenovic A., Malina J., (2013), Adsorption ability of carbon black for nickel ions uptake from aqueous solution, *Hemijaska Industrija*, **67**, 51-58.
- Radjenovic A., Medunic G., (2015), Removal of Cr(VI) from aqueous solution by a commercial carbon black, *Desalination and Water Treatment*, **55**, 183-192.
- Rafatullah M., Sulaiman, O., Hashim, R., Ahmad, A., (2009), Adsorption of copper (II), chromium (III), nickel (II) and lead (II) ions from aqueous solutions by meranti sawdust, *Journal of Hazardous Materials*, **170**, 969-977.

- Srinivasan M.P., Yaming N., (2001), Novel activation process for preparing highly microporous and mesoporous activated carbon, *Carbon*, **39**, 877-886.
- Srivastava V., Gusain D., Bux F., Sharma G.C., Sharma Y.C., (2017), Optimization of important process parameters for the removal of Cr(VI) by a modified waste material, *Environmental Engineering and Management Journal*, **16**, 2719-2730.
- Sud D., Mahajan G., Kaur M.P., (2008), Agricultural waste material as potential adsorbent for sequestering heavy metal ions from aqueous solutions: A review, *Bioresource Technology*, **99**, 6017-6027.
- Štrkalj A., Radjenović A., Malina J., (2010), The use of metallurgical waste material from aluminium production for the removal of chromium (VI) ions from aqueous solutions, *Archives of Metallurgy and Materials*, **55**, 449-454.
- Ünlü N., Ersoz M., (2007), Removal of heavy metal ions by using dithiocarbamated-sporopollenin, *Separation and Purification Technology*, **52**, 461-469.
- Wang X.S., Chen L.F., Li F.Y., Chen K.L., Wan W.Y., Tang Y.J., (2010), Removal of Cr(VI) with wheat-residue derived black carbon: Reaction mechanism and adsorption performance, *Journal of Hazardous Materials*, **175**, 816-822.
- Weber Jr W.J., Morris J.C., (1963), Kinetics of adsorption on carbon from solution, *Journal of the Sanitary Engineering Division*, **89**, 31-59.
- Yao Z.-Y., Qi J.-H., Wang L.-H., (2010), Equilibrium, kinetic and thermodynamic studies on the biosorption of Cu(II) onto chestnut shell, *Journal of Hazardous Materials*, **174**, 137-143.